

NEW ELECTROPRODUCTION RESULTS FROM DESY

H. Spitzer
Universität Hamburg
II. Institut für Experimentalphysik



Abstract

We review recent electroproduction results from DESY above the resonance region ($W > 1.7$ GeV) in the framework of a quark-parton model. ρ^0 and ω production off protons has stronger nonperipheral contributions than in photoproduction. The ρ/ω cross section ratios as well as the ratio of single π^- and π^+ production off deuterons approach the quark model values at $|t| \sim 1$ GeV² and at values of the scaling variable ω of 4 - 7. Inclusive production of π^- mesons via $\gamma_{\nu}p \rightarrow \pi^-X$ is suppressed in the fragmentation region, whereas the production of 1 prong events of the type $\gamma_{\nu}p \rightarrow \pi^+n\pi^0 \dots$ is much stronger than in photoproduction. Both observations are compatible with a preferred production of leading positive mesons when the virtual photon hits a valence quark inside the proton. New measurements of the reactions $\gamma_{\nu}p \rightarrow \pi^+n$ and $\gamma_{\nu}p \rightarrow \pi^0p$ allow a separation of the longitudinal cross sections. A further analysis shows that the transverse cross section σ_{\perp} dominates over σ_{\parallel} in the same way as in photoproduction.

1. INTRODUCTION

This report covers new results on electroproduction which were recently obtained at DESY. In spite of the effort put on storage ring experiments, there are still some healthy electroproduction experiments going. What kind of physics can you expect in inelastic ep scattering at DESY energies? Let us first have a look at the kinematic region of electroproduction* (see fig. 1). The region is limited by photoproduction ($Q^2 = 0$) on the one

DESY

26082

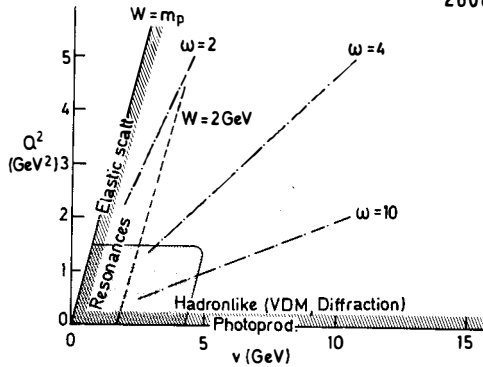


Fig. 1. The kinematical region ($Q^2 - \nu$ plane) of inelastic ep scattering and elastic ep scattering ($W =$ proton mass m_p) on the other hand. What reaction mechanisms do we expect near these limits? We know from previous experiments that s -channel resonances can be excited at $W < 2$ GeV. Also at small Q^2 diffractive processes like quasielastic ρ and ω production take place, which can be described by a vector dominance approach. In general the interaction at small Q^2 is thought to be hadronlike:

* The kinematic quantities used are $-Q^2 =$ "mass squared" of the virtual photon, which mediates the ep interaction, $\nu =$ energy of the virtual photon in the lab. system, $W =$ total energy of the γ_p center of mass system.

We further know that the total inelastic ep scattering cross section develops an approximate scaling behaviour for $Q^2 > 1 \text{ GeV}^2$ and $W > 2 \text{ GeV}$. The first observation of this behaviour gave a boost to quark parton models for deep inelastic scattering. Usually deep inelastic effects are expected only for small values of the scaling variable $\omega = \frac{2 m_p \nu}{Q^2}$, i.e. $\omega < 4$ and both Q^2 and ν large. The dot dashed lines in fig. 1 indicate lines of constant ω . The shaded area in fig. 1 indicates the kinematic region accessible to typical experiments at DESY. Part of the region has small ω .

Hence we can explore a region, where on the one hand hadronlike processes take place and where on the other hand the scaling behaviour is taking over. The question is, if the early onset of scaling is accompanied by any observable quark-parton effects.

In this talk I will not cover the resonance region below $W = 1.7 \text{ GeV}$. I want to focus on two questions:

- Do valence quarks effect the reaction dynamics?

We have indications that this might happen in our $Q^2 - W$ range at large $|t|$ (for two-body reactions) and in the fragmentation region (for inclusive distributions).

- Do the reaction dynamics for single π production at small t and moderate Q^2 differ from photoproduction?

Table 1 gives a survey of the reactions which were recently measured at DESY.

The streamer chamber data cover mainly vector meson production and inclusive distributions¹⁻⁴ at values of the polarisation parameter $\epsilon = 0.85-0.95$.

A small data sample was also taken at $\epsilon = 0.35 - 0.5$ ⁵. There is high quality data on single π^+ and π^- production off hydrogen and deuterium at large ϵ ^{6,8}. Two groups have measured single π^+ production at $\epsilon \approx 0.4$, which allows a separation of longitudinal and transverse contributions^{7,9}.

TABLE 1

Survey of recent electroproduction data from DESY above the resonance region ($W > 1.7$ GeV)

Collaboration	Channel	Kinematic Range					Ref.
		W [GeV]	Q ² [GeV ²]	ε	t [GeV ²]		
DESY-Glasgow-	$\gamma_{\nu P} \rightarrow \rho P$	1.7 - 2.8	0.3 - 1.4	0.85 - 0.95	≤ 2	1	
Hamburg	$\gamma_{\nu P} \rightarrow \omega P$					2	
(Streamer Chamber)	$\gamma_{\nu P} \rightarrow \pi^- \Delta^{++}$					1,3	
Chamber)	$\gamma_{\nu P} \rightarrow \pi^- X$	2.2 - 2.8	0.3 - 1.4	0.84	(-1 < x < 1)	4	
		~3	0 - 2	~0.4	(-1 < x < 1)	5	
	$\langle n_{ch} \rangle$,	1.3 - 2.8	0.3 - 1.4	0.8 - 0.98	-	4	
	topol. cross sections	3 - 3.5	0 - 1	0.35 - 0.5	-	5	
DESY (Group	$\gamma_{\nu P} \rightarrow \pi^+ n$	2.19	0.06 - 1.35	0.76 - 0.86	$t_{min} -1.0$	6	
F22)-Univ.		2.19	0.7	0.33	0.05-0.24	7	
Hamburg	$\gamma_{\nu n} \rightarrow \pi^- p$	2.19	0.7, 1.35	0.85	$t_{min} -1.0$	8	
DESY (Group	$\gamma_{\nu P} \rightarrow \pi^+ n$	2.08 - 2.2	0.2 - 0.55	0.35 - 0.45	0.02 - 0.2	9	
F32)-Wuppertal							
Aachen-DESY-	$\gamma_{\nu P} \rightarrow \pi^0 P$	1.8 - 2.5	0.1 - 0.6	0.5	0.05-0.7	10	
Wuppertal				$\langle \phi \rangle = 15^\circ$			
	$\gamma_{\nu P} \rightarrow \pi^0 X$	1.8 - 3.5		0.35 - 0.8	(0.4 < x < 1)	10	

Finally an Aachen-Wuppertal-DESY collaboration has measured π^0 production both via $\gamma_{\nu p} \rightarrow \pi^0 p$ and $\gamma_{\nu p} \rightarrow \pi^0 X$ $\times 10$.

The total amount of data is too large to be covered in this report. In view of the above questions I want to concentrate on the following topics:

- Summary of peripheral ρ^0 and ω production (sec. 2).
- Nonperipheral ρ^0 and ω production (sec. 3).
- Quark-Parton effects in $R = \frac{\sigma(\gamma_{\nu n} \rightarrow \pi^+ p)}{\sigma(\gamma_{\nu p} \rightarrow \pi^+ n)}$ (sec. 4).
- Q^2 dependence of nonperipheral production (sec. 5).
- Suppression of π^- production in the fragmentation region (sec. 6).
- How is the total cross section built up from individual channels? (sec. 7).
- Separation of longitudinal and transverse contributions to $\gamma_{\nu p} \rightarrow \pi^+ n$ and $\gamma_{\nu p} \rightarrow \pi^0 p$ (sec. 8).

2. Summary of peripheral ρ and ω production

The streamer chamber experiment has yielded a clear picture of ρ and ω production via $\gamma_{\nu p} \rightarrow \rho p$ or $\gamma_{\nu p} \rightarrow \omega p$ in our Q^2 -W range. These are the main observations ^{1,2}:

- 1) The ρ and ω production cross section has a strong peripheral component with exponential slopes similar to those measured in photoproduction.
- 2) The W dependence of the peripheral cross section is well compatible with a diffractive process for ρ production and a mixture of one-pion-exchange (OPE) and diffractive contributions for ω production.
- 3) Other properties of ρ production (like dominance of natural parity exchange and s-channel helicity conservation) are similar to those found in photoproduction.
- 4) The cross section drops fast between $Q^2 = 0$ and $Q^2 = 0.3 \text{ GeV}^2$ in agreement with a vector dominance model calculation. (See fig. 2, which shows the reaction cross section normalized to the total cross section.)

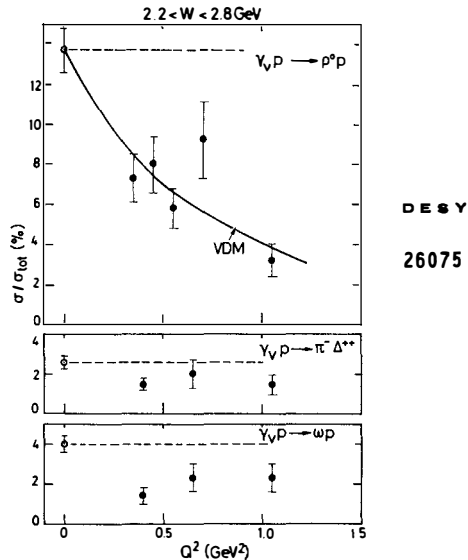


Fig. 2 Reaction cross sections normalized to the total inelastic ep cross section as a function of Q^2 . The full points and VDM curve are from refs. 1 and 2.

In summary, peripheral ρ and ω electroproduction can be well understood (in our $Q^2 - W$ range) by the same mechanisms as in photoproduction. The observed Q^2 dependence is governed by the p propagator. In contrast the nonperipheral production shows a much weaker Q^2 dependence.

3. Nonperipheral ρ and ω production

To look for nonperipheral contributions we plot in fig. 3 the differential cross sections $d\sigma/dQ$ in the hadronic center of mass system above threshold ($1.7 < W < 2.0$ GeV). We observe the following main features:

- 1) The distributions have the above mentioned peripheral peaks near $\cos \theta_{\text{cm}} = 1$ both in electroproduction (full points) and photoproduction (open points).

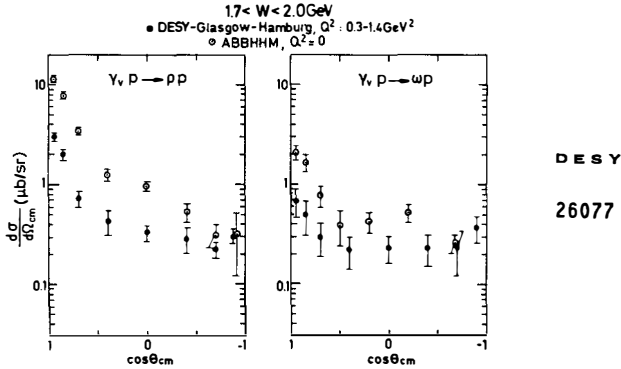


Fig. 3 Differential cross sections in the hadronic center of mass system for $\gamma_p \rightarrow \rho^0 p$ and $\gamma_p \rightarrow \omega p$ at $\langle Q^2 \rangle = 0.75 \text{ GeV}^2$ from refs. 1 and 2, which also contain references of the photoproduction points.

- 2) ρ and ω electroproduction develops a nearly isotropic production angular distribution for $\cos \theta_{\text{cm}} < 0.5$.
- 3). The ratio of ρ to ω production becomes close to 1 in the backward hemisphere both in electroproduction and photoproduction.
- 4). In the backward hemisphere there is little drop of the cross sections between $Q^2 = 0$ and $\langle Q^2 \rangle = 0.75 \text{ GeV}^2$.

In summary, we find strong nonperipheral contributions of comparable size in ρ and ω electroproduction near threshold which have a weak Q^2 dependence. These can be caused by the formation of $J = \frac{1}{2}$ or $J = \frac{3}{2}$ s-channel resonances¹ or by some presently unknown processes.

Let us look if the observed phenomena persist at higher energies. Fig. 4 shows the differential cross sections $d\sigma/dt$ for ρ (open triangles) and ω production (full points). The average value of the scaling variable is $\omega \sim$

7 for the electroproduction data. Again the nonperipheral cross sections (for $|t| > 0.5 \text{ GeV}^2$) are within errors of comparable size.

DESY

26070

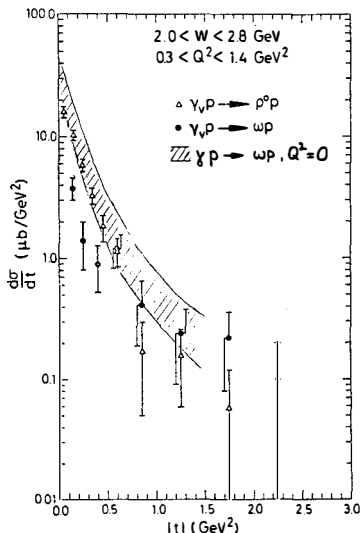


Fig. 4 Differential cross sections $d\sigma/dt$ for reactions $\gamma_V p \rightarrow \rho^0 p$ (open triangles) and $\gamma_V p \rightarrow \omega p$ (full points) from refs. 1 and 2. The shaded area indicates the photoproduction cross section for $\gamma p \rightarrow \omega p$, as quoted in ref. 2.

The last observation can be understood in the framework of a simple quark model. Let us assume that nonperipheral ρ and ω production is initiated by a virtual photon coupling to a valence quark of the proton. Since both ρ and ω have the same quark content one would then expect equal amounts of ρ and ω production.

$$4. \text{ Quark-Parton effects in } R = \frac{\sigma(\gamma_V n \rightarrow \pi^- p)}{\sigma(\gamma_V p \rightarrow \pi^+ n)}$$

There is another example where we can look for quark parton effects. Consider the reactions $\gamma_V n \rightarrow \pi^- p$ and $\gamma_V p \rightarrow \pi^+ n$. According to Nachtmann¹¹ one

would expect that photon-valence quark interactions dominate for a) $\omega \ll 5$ and b) transverse photons only. The latter condition is realized at high $|t|$, since longitudinal photons contribute mostly at low $|t|$ via OPE (compare fig. 14) and play little role at high $|t|$. Fig. 5 shows the relevant quark diagrams.

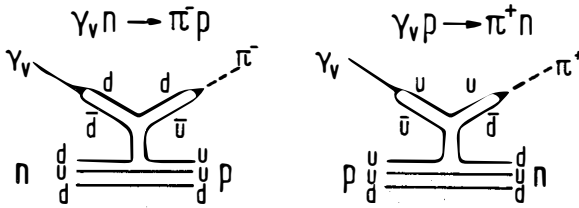


Fig. 5 Quark graphs for $\gamma_V n \rightarrow \pi^- p$ and $\gamma_V p \rightarrow \pi^+ n$

The amplitude for π^- production is proportional to the charge $-\frac{1}{3}$ of the d quark, from which the π^- is formed, whereas the π^+ production amplitude is proportional to the charge of the u quark $\frac{2}{3}$. Hence we expect a ratio of the production cross sections of $R = \frac{1}{4}$. Fig. 6 shows the ratio of single π^- to π^+ production off deuterons⁸, which apart from small deuterium effects is equal to the above ratio R . The data have values of $\omega = 6.7$ ($Q^2 = 0.7 \text{ GeV}^2$) and $\omega = 4$ ($Q^2 = 1.35 \text{ GeV}^2$), respectively. Near $t = 0$ where the production mechanism is dominated by OPE the ratio is close to 1 (as in photoproduction (shaded area)), whereas for $|t| > 0.5 \text{ GeV}^2$ the ratio R approaches the value $\frac{1}{4}$ expected from the quark model.

Hence the data on the ρ/ω and the π^-/π^+ ratio are consistent with valence quark effects at kinematic values $|t| \approx 1 \text{ GeV}^2$, $Q^2 \approx 1 \text{ GeV}^2$ and $\omega \approx 4-7$. Let us now ask for the Q^2 dependence of nonperipheral processes.

5. Q^2 dependence of nonperipheral production

In this section we consider three two-body reactions: $\gamma_V p \rightarrow \omega p$, $\gamma_V p \rightarrow \pi^- \Delta^{++}$ and $\gamma_V p \rightarrow \pi^+ n$ at large t . The full points in fig. 4 give the differential

cross sections for ω production at energies $2.0 < W < 2.8$ GeV. The shaded area indicates the photoproduction differential cross section for $\gamma p \rightarrow \omega p$. At small $|t|$ the photoproduction cross sections exceed the ω electroproduction data, which have an average $\langle Q^2 \rangle = 0.84$ GeV². In contrast, the photoproduction and electroproduction cross sections are of the same magnitude for $|t| > 0.5$ GeV², i.e. they show no significant Q^2 dependence.

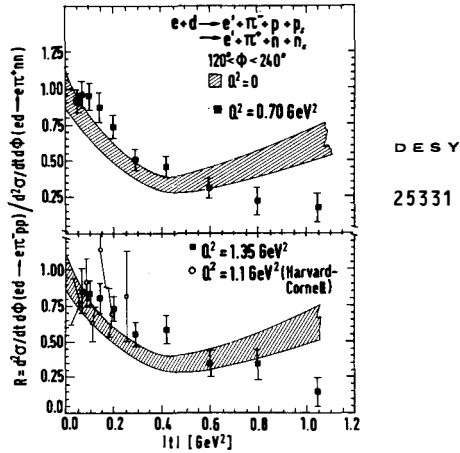


Fig. 6 The ratio R of single π^- production to single π^+ production cross sections off deuterium at $Q^2 = 0.7$ ($\omega = 6.7$) and $Q^2 = 1.35$ GeV² ($\omega = 4$). The figure was taken from ref. 8.

The same observation is made in fig. 7., where full points are from electroproduction of $\pi^- \Delta^{++}$ and open points are from photoproduction. Finally fig. 8 shows the double differential cross section $2 \pi d^2 \sigma / dt d\phi$ for the reaction $\gamma_p p \rightarrow \pi^+ n$ at $W = 2.19$ GeV* and four different Q^2 values. The shaded area indicates the corresponding photoproduction cross sections. Let us discuss the data at $Q^2 = 0.7$ GeV².

* See next page for footnote

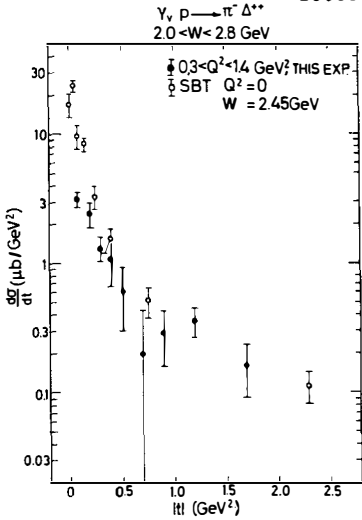


Fig. 7 The differential cross section $d\sigma/dt$ for $\gamma_V p \rightarrow \pi^- \Delta^{++}$ from ref. 3 (full points). The open points (photoproduction) are from ref. 12.

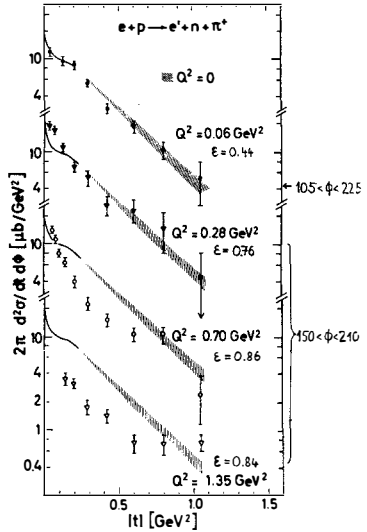


Fig. 8 Differential cross section for $\gamma_V p \rightarrow \pi^- n$ at $W = 2.19$ GeV from ref. 6. The cross sections have been averaged over the indicated ϕ range.

At small $|t|$ the electroproduction cross section exceeds the photoproduction data, due to strong longitudinal contributions, which die out fast with increasing $|t|$. For $|t| > 0.7$ GeV² the electroproduction cross sections approach again the photoproduction values. Similar trends are observed at Q² values of 0.28 and 1.35 GeV².

* Here ϕ is the angle between the electron scattering plane and the π^+ production plane, spanned by the momentum vectors of the γ_V and π^+ . The cross sections were averaged over the indicated ϕ regions. Averaging over the full ϕ range would yield slightly higher cross sections, since the cross section is minimal for $\phi = 0^\circ, 180^\circ, 360^\circ$ and maximal for $\phi = 90^\circ, 270^\circ$.

In conclusion, we have found that the reactions $\gamma_{\nu} p \rightarrow \omega p$, $\gamma_{\nu} p \rightarrow \pi^{-} \Delta^{++}$ and $\gamma_{\nu} p \rightarrow \pi^{+} n$ show little Q^2 dependence at $|t| \approx 0.7 \text{ GeV}^2$. Note that the average ω of the electroproduction data is of the order of 4 - 7. A weak Q^2 dependence of the cross section is reminiscent of a pointlike interaction in the framework of a quark-parton model, though certainly other explanations of the observed phenomena can be found.

6. Suppression of π^{-} production in the fragmentation region

We next turn to the π^{-} inclusive distributions from the streamer chamber experiment. We ask if quark-parton effects can be observed in the fragmentation region. If the π^{-} in the fragmentation region are produced by a γ_{ν} hitting a valence quark one would expect a suppression of π^{-} production relative to π^{+} production, as soon as this mechanism turns on*. We plot the inclusive distributions as a function of the variable $x = p_{\parallel}^{*} / p_{\parallel}^{* \text{ max}}$, and where p_{\parallel}^{*} is the π^{-} longitudinal momentum in the hadronic center of mass system and $p_{\parallel}^{* \text{ max}}$ is its maximal value. The left hand side of fig. 9 shows the structure

$$\text{function } F(x) = \frac{1}{\pi \sigma_{\text{tot}}} \int_0^{\infty} \frac{E^{*}}{p^{* \text{ max}}} \frac{d^2}{dx dp_{\perp}^2} dp_{\perp}^2 \quad (1)$$

for energies $2.2 < W < 2.8 \text{ GeV}$. Full points are for $0.3 < Q^2 < 0.5 \text{ GeV}^2$ and open points for $0.5 < Q^2 < 1.4 \text{ GeV}^2$. The curve indicates the corresponding distribution for photoproduction^{13**}. In the target fragmentation region ($x < 0$) the data develop no significant Q^2 dependence between $Q^2 = 0$ and $Q^2 = 1 \text{ GeV}^2$,

* The suppression is due to the small charge of the d quark, which is necessary to form a π^{-} , by the same argument as discussed in sec. 4.

** The peak in the photoproduction distribution near $x = 0.9$ is due to the reaction $\gamma p \rightarrow \pi^{-} \Delta^{++}$.

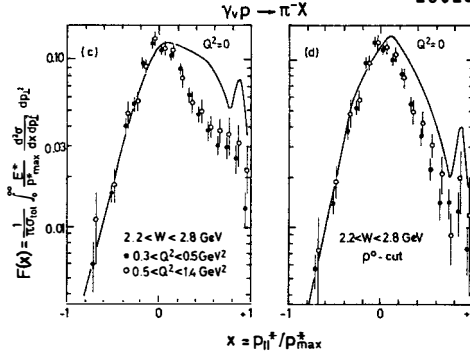


Fig. 9 The structure function $F(x)$ for $\gamma_{\nu} p \rightarrow \pi^- X$ from ref. 4. The righthand part has all events fitting reaction $\gamma_{\nu} p \rightarrow \pi^+ \pi^- p$ with $M_{\pi^+ \pi^-} < 1 \text{ GeV}$ removed. The curve is an interpolation through the corresponding photoproduction data of ref. 13 at $W = 2.45 \text{ GeV}$.

which indicates that the target fragmentation is approximately independent of the projectile mass. In contrast we observe a sharp drop of $F(x)$ in the beam fragmentation region ($x \gtrsim 0.3$) between $Q^2 = 0$ and $\langle Q^2 \rangle = 0.4 \text{ GeV}^2$. A similar drop has not been observed in inclusive π^+ production¹⁴.

We might ask if the drop is caused by the fast disappearance of diffractive ρ production when moving from $Q^2 = 0$ to $\langle Q^2 \rangle = 0.4 \text{ GeV}^2$ (compare fig. 2). In order to check this question we have plotted in the right hand part of fig. 9 $F(x)$ with all ρ^0 events removed from the data both in photo- and electroproduction. The discrepancy between photo- and electroproduction is reduced by a factor 1.5, but does not disappear completely. Other known diffractive processes (like $\gamma p \rightarrow \omega p$ or diffractive $\gamma p \rightarrow \rho^0 X$) are too weak to come up for the remaining difference. Hence the suppression of π^- production in the fragmentation region is consistent with being partially due to quark-parton effects. It is surprising that such effects show up at small Q^2 immediately after the photon "becomes" virtual.

7. How is the total inelastic cross section built up from individual channels?

Ever since the surprisingly weak Q^2 dependence of the total inelastic cross section was found, experimenters have tried to find out which channels are responsible for this behaviour. The streamer chamber experiment can shed a bit more light on the question. We first look at the topological cross sections σ_n for the production of n charged hadrons normalized to the total inelastic cross section. Fig. 10 shows σ_n/σ_{tot} as a function of Q^2 for $2.2 < W < 2.8$ GeV. As already observed in previous experiments ^{15, 16}, the data show a remarkable independence of Q^2 . However, there is a marked

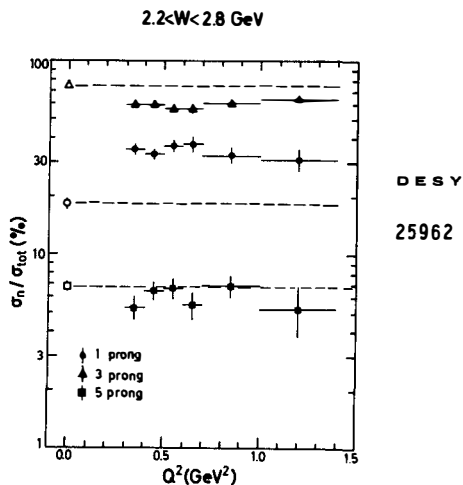


Fig. 10 Topological cross sections for $\gamma_{\nu} p \rightarrow n$ charged particles normalized to the total inelastic ep cross section from ref. 4.

transition when moving from photoproduction (open points) to electroproduction (full points). The fraction of 3 prong events is reduced, whereas the fraction of 1 prong events sharply increases and the fraction of 5 prong events stays approximately constant. The reduction of σ_3/σ_{tot} can be partially (but not fully) explained by the dying out of diffractive ρ and ω production ⁴.

We might ask if the increase of 1 prongs is caused by contributions from longitudinal photons in reactions like $\gamma_{\nu}p \rightarrow \pi^+n$ or $\gamma_{\nu}p \rightarrow \pi^0p$. In order to study this question we plot in fig. 11 the missing mass squared MM^2 of the neutral system produced in one prong events. Clear peaks are observed at $MM^2 = M_{\pi^0}^2$ and $MM^2 = M_n^2$ corresponding to the reactions $\gamma_{\nu}p \rightarrow \pi^0p$ and $\gamma_{\nu}p \rightarrow \pi^+n$. However, the vast majority of the events occurs at higher values of MM^2 , which implies the production of additional neutral particles.

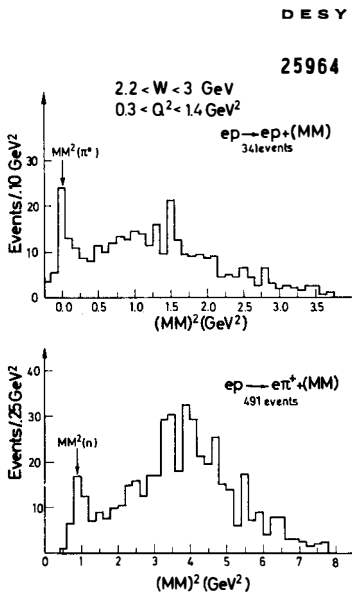


Fig. 11 Missing mass squared distributions for 1 prong events from ref. 4.

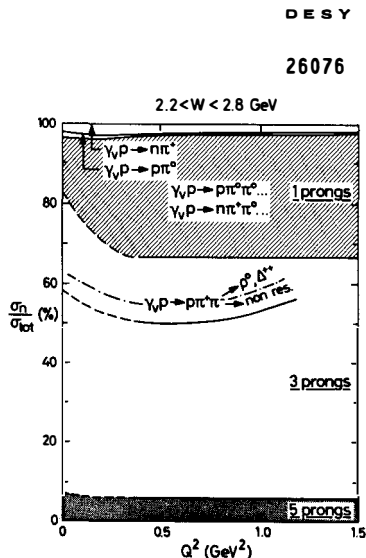


Fig. 12 Channel cross sections normalized to the total cross section. The cross section for $\gamma_{\nu}p \rightarrow \pi^+\pi^-$ is from ref. 1.

The cross sections for $\gamma_{\nu}p \rightarrow n\pi^+$ and $\gamma_{\nu}p \rightarrow p\pi^0$ were estimated from the data presented in figs. 8 and 16.

We have estimated the cross sections for $\gamma_{\nu p} \rightarrow \pi^0 p$ and $\gamma_{\nu p} \rightarrow \pi^+ n$ from our data and the data presented in sec. 8. The result is indicated in fig. 12, where we again show fractional cross sections vs. Q^2 . Clearly the above two-body final states cannot explain the strong increase in the 1 prong cross section. It is caused by 1 prong events with two or more neutral particles.

If the increase would be mainly due to nonresonant events of the type $\gamma_{\nu p} \rightarrow p \pi^0 \pi^0$ we would expect a similar increase in the fraction of nonresonant events $\gamma_{\nu p} \rightarrow p \pi^+ \pi^-$, which are also indicated in fig. 12. This is not observed. We conclude that most likely events of the type $\gamma_{\nu p} \rightarrow \pi^+ n \pi^0 \dots$ are responsible for the increased 1 prong fraction. This observation does fit in the quark-parton model which favours the production of positive charged mesons like π^+ or ρ^+ in the fragmentation region.

When such mesons are produced the remaining energy is in our W range - frequently not large enough to create additional $\pi^+ \pi^-$ pairs. We expect that at higher W the excess of 1 prong events slowly will disappear whereas other channels with leading positive mesons like $\gamma_{\nu p} \rightarrow \pi^+ \pi^+ \pi^- n$ take over.

While our observation fits in the quark-parton model it is again surprising that the excess of 1 prongs is "turned on" already at very small values of Q^2 .

8. Separation of longitudinal and transverse contributions

to $\gamma_{\nu p} \rightarrow \pi^+ n$ and $\gamma_{\nu p} \rightarrow \pi^0 p$

We now turn to a different subject, namely single π production at small Q^2 and t and ask, whether the interaction shows similarities to photoproduction.

Single π electroproduction offers the possibility to disentangle the contributions of different spin states of the virtual photon as one can see from the differential cross section formula

$$2\pi \frac{d^2\sigma(\gamma_p p \rightarrow \pi N)}{dt d\phi} = \frac{d\sigma_U}{dt} + \epsilon \frac{d\sigma_L}{dt} + \epsilon \cos 2\phi \frac{d\sigma_P}{dt} + \sqrt{2\epsilon(\epsilon+1)} \cos\phi \frac{d\sigma_I}{dt} \quad (2)$$

There are four contributions to the cross section:

$\sigma_U = \frac{1}{2}(\sigma_{\parallel} + \sigma_{\perp})$ from transverse unpolarized photons (as in unpolarized photoproduction); σ_{\parallel} and σ_{\perp} are the cross sections corresponding a polarization of the photon electric vector parallel and perpendicular to the reaction plane, respectively.

σ_L from longitudinal photons.

$\sigma_P = \frac{1}{2}(\sigma_{\parallel} - \sigma_{\perp})$ from the interference of the two transversely polarized photon components.

σ_I from the interference of amplitudes due to transverse and longitudinal photons

ϵ is the polarization parameter*. The azimuthal angle ϕ was defined in sec. 5 (footnote).

The measurement of the ϕ dependence of the cross section allows the separation of $(\sigma_U + \epsilon\sigma_L)$, σ_P and σ_I . Measurements at fixed Q^2 , W and t but at different ϵ separate σ_U from σ_L .

A DESY-University Hamburg group ^{6,7} has performed such measurements at $W = 2.19$ GeV and $Q^2 = 0.7$ GeV² for $\gamma_p p \rightarrow \pi^+ n$. Fig. 13 shows the separated contributions

$$\frac{d\sigma_U}{dt} + \epsilon \frac{d\sigma_L}{dt}, \frac{d\sigma_P}{dt} \text{ and } \frac{d\sigma_I}{dt}.$$

The contribution of $\sigma_U + \epsilon\sigma_L$ dominates at small t , showing a drastic t dependence. Fig. 14 (top) shows the separated cross sections σ_L (open diamonds) and σ_U (full circles). The data demonstrate clearly that it is the

* $\epsilon = [1 + 2 \tan^2 \frac{\theta}{2} (1 + \frac{v^2}{Q^2})]^{-1}$ with θ = electron scattering angle in the lab. system. The transverse part of the virtual photon is polarized to degree ϵ , with the polarization vector in the electron scattering plane. The longitudinal polarization component has a total intensity ϵ times the total intensity in the transverse components.

longitudinal cross section, which causes the sharp drop of the overall

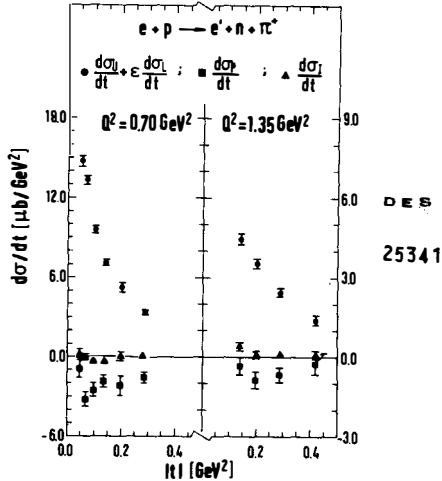


Fig. 13 Differential cross sections $d\sigma_U/dt + \epsilon d\sigma_I/dt$, $d\sigma_P/dt$ and $d\sigma_I/dt$ for reaction $\gamma_p p \rightarrow \pi^+ n$ at $W = 2.19$ GeV and $\langle \epsilon \rangle = 0.85$ (from ref. 6).

cross section with increasing $|t|$. This behaviour can be fitted by a generalized Born term model of Gutbrod and Kramer¹⁷ (curves in fig. 14), in which π exchange contributions dominate the longitudinal cross section. We can go one step further and isolate σ_{\perp} and σ_{\parallel} by resolving σ_U and σ_P .

Fig. 15 shows σ_{\perp} and σ_{\parallel} at $Q^2 = 0.7$ GeV² as a function of t . The curves indicate the corresponding cross sections in photoproduction, divided by an arbitrary factor 3 to compensate the Q^2 dependence. σ_{\perp} and σ_{\parallel} have approximately the same properties as in photoproduction*. σ_{\perp} dominates and has a similar t dependence as at $Q^2 = 0$. The observation of a forward peak in σ_{\parallel} is precluded by the large value of t_{\min} at $Q^2 = 0.7$ GeV².

* σ_{\perp} and σ_{\parallel} are at high W characterized by a unique naturality of the t -channel exchange: natural parity exchange ($J^P = 0^+, 1^-, \dots$) only for σ_{\perp} and unnatural parity exchange ($J^P = 0^-, 1^+, \dots$) for σ_{\parallel} ¹⁸.

26080

26078

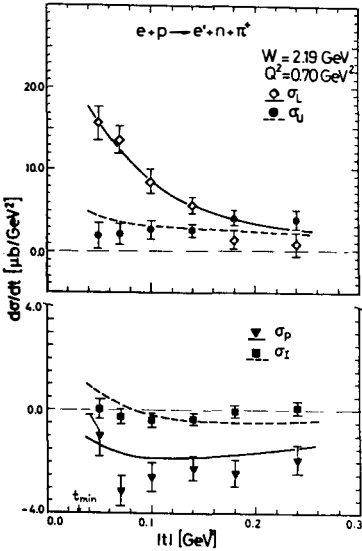


Fig. 14 Separated differential cross sections $d\sigma_U/dt$, $d\sigma_L/dt$, $d\sigma_P/dt$ and $d\sigma_T/dt$ for $\gamma_V p \rightarrow \pi^+ n$ (from ref. 7). The curves are fits using a Born term model of Gutbrod and Kramer¹⁷.

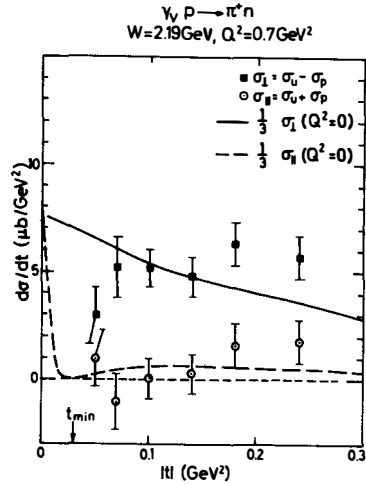


Fig. 15 Differential cross sections $d\sigma_I/dt$ and $d\sigma_{II}/dt$ for $\gamma_V p \rightarrow \pi^+ n$ (from ref. 7). The curves indicate the corresponding photoproduction cross sections¹⁹ taken at $E_\gamma = 3.4$ GeV and scaled down by $(s-M_p^2)^2$ to $W = 2.19$ GeV.

In addition the photoproduction cross sections were divided by a factor 3.

We finally consider single π^0 production $\gamma_V p \rightarrow \pi^0 p$. Here a small σ_L is expected for the following reasons:

- 1) Pion exchange is forbidden by C conservation
- 2) The dominant exchange expected is the ω , a natural parity exchange which does not contribute to σ_L at high W .

Fig. 16 shows the recently measured differential cross sections at an average ϕ of 15° (full points¹⁰) together with the 1975 data taken at an average ϕ of 90° . The cross sections at $\phi=90^\circ$ are larger by a factor two than the 15° cross sections. The observed strong ϕ dependence requires σ_p to be large and negative (see eq. (2), i.e. $\sigma_\perp \gg \sigma_\parallel$).

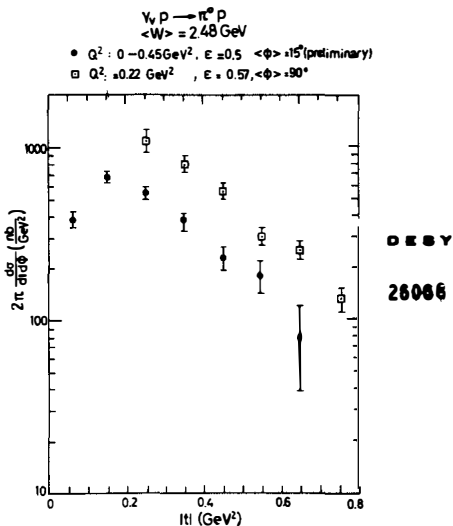


Fig. 16 Double differential cross sections for reaction $\gamma_p \rightarrow \pi^0 p$. Full points are from ref. 10 ($\langle\phi\rangle = 15^\circ$). Open points are from table 4 of ref. 20 ($\langle\phi\rangle = 90^\circ$) scaled down from $W = 2.56$ GeV to $W = 2.48$ GeV.

By assuming σ_L and σ_\perp to vanish one can extract σ_p , and further on extract σ_\perp and σ_\parallel from σ_U and σ_p . The cross sections $\frac{d\sigma_\perp}{dt}$ and $\frac{d\sigma_\parallel}{dt}$ at $Q^2 = 0.22$ GeV² are shown in fig. 17. The corresponding cross sections from photo-production are shown in fig. 18. In both cases σ_\perp dominates over σ_\parallel .

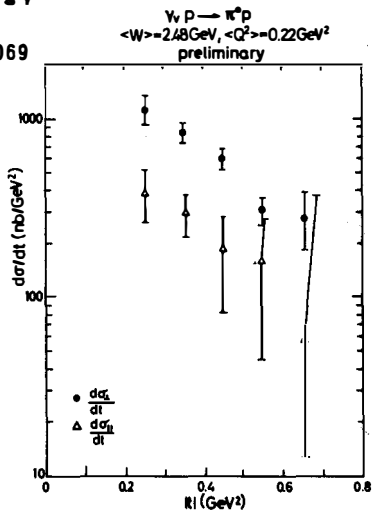


Fig. 17 Separated differential cross sections $d\sigma_{\perp}/dt$ and $d\sigma_{\parallel}/dt$ for reaction $\gamma p \rightarrow \pi^0 p$ using the data of ref. 10 and ref. 20.

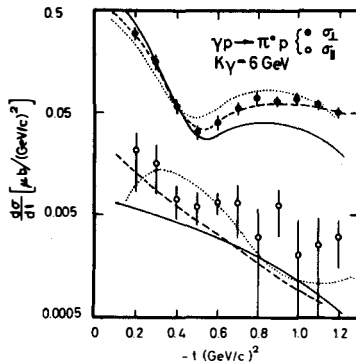


Fig. 18 Separated differential cross sections $d\sigma_{\perp}/dt$ and $d\sigma_{\parallel}/dt$ for photoproduction $\gamma p \rightarrow \pi^0 p$ (from ref. 21).

In summary, the transverse contributions to single π^+ and π^0 electroproduction are dominated by the cross section due to natural parity exchange. This is qualitatively the same behaviour as in photoproduction.

Acknowledgement: I thank C. Berger, T. Ganzler, W. Gabriel and M. Helm for communicating to me unpublished results of their groups. I am indebted to the members of the DESY-Glasgow-Hamburg collaboration for a long and fruitful cooperation. Part of this work was supported by the Bundesministerium für Forschung und Technologie.

References

1. P. Joos et al., Nucl. Phys. B113 (1976) 53
2. P. Joos et al., DESY Report 77/09 (1977), submitted to Nucl. Phys. B
3. K. Wacker, Thesis, Internal Report DESY F1-76/04 (1976) (unpublished)
4. C. K. Chen et al., to be published
5. J. Knobloch, Thesis, Internal Report DESY F1-76/03 (1976)(unpublished)
6. P. Brauel et al., DESY Report 76/33 (1976),
P. Brauel et al., Phys. Letters 65 B (1976) 181
7. P. Brauel et al., to be published
8. P. Brauel et al., Phys. Letters 65 B (1976) 184,
M. Schädlich, Thesis, Internal Report DESY F22-76/02 (1976) (unpublished)
9. DESY-Wuppertal collaboration, private communication
10. Aachen-DESY-Wuppertal collaboration, private communication from C.
Berger
11. O. Nachtmann, Nucl. Phys. B115 (1976) 61
12. J. Ballam et al., Phys. Rev. D5 (1972) 545
13. K. Moffeit et al., Phys. Rev. D5 (1972) 1603
14. J. Ballam et al., Contribution to the 6th International Symposium on
Electron and Photon Interactions at High Energies, Bonn (1973), see
p. 262 of the Symposium Proceedings, North Holland Publ. Comp., 1974,
ed. by H. Rollnik and W. Pfeil
15. J. Ballam et al., Phys. Letters 56B (1975) 193
16. C. del Papa et al., Phys. Rev. D13 (1976) 2934
17. F. Gutbrod and G. Kramer, Nucl. Phys. B49 (1972) 461
18. P. Stichel, Zeitschr. f. Phys. 180 (1964) 170; J. P. Ader et al.,
Nuovo Cim. 56A (1968) 952
19. K. Lübbelsmeyer, Proc. of the 4th Intern. Symposium on Electron and
Photon Interactions at High Energies, Liverpool 1969, ed. by D. W.
Braben

20. K. H. Me β , Thesis, Internal Report DESY F35-75/1 (1975) (unpublished)
The cross section σ_{\perp} extracted from the data is given in F. W. Brasse
et al., Phys. Letters 58B (1975), 467
21. B. Wiik, Proc. of the 1971 International Symposium on Electron and
Photon Interactions at High Energies, Cornell University, Ithaca, N.Y.
(1971), ed. by N. B. Mistry